

# To Assess Radiation Susceptibility of Semiconductor Devices Base on Similarity Principle

Hongmin Liu<sup>1</sup>, Weng Zheng<sup>1</sup>, Ruixuan Li<sup>1</sup>, Jiaqiang Liu<sup>1</sup>, Shuai Cui<sup>2</sup>

1.National Space Science Center, CAS, Beijing, China

+8601062582695, rel-center@nssc.ac.cn

2. Innovation Academy for Microsatellite, CAS, Shanghai, China

+8602120857000-83011, cshuai@eyou.com

**Abstract**—Electronic parts in space inevitably subject to radiation effects leading to the degradation of electronic performance or even failure, so radiation performance of an electronic part must be assessed to ensure it work normally in space. At present, to assess the ion radiation effects on a semiconductor device is directly through irradiation tests. However, due to the scarcity of cyclotron resources, the test time is difficult to appoint and the cost is huge. Due to schedule and budget constraints, it is also impossible to conduct irradiation tests on all semiconductor devices in actual space missions. Therefore, assessment of the radiation effects on semiconductor devices through irradiation tests has caused difficulties. Radiation susceptibility of semiconductor device is determined by the design topology and fabrication technology, and the irradiation test data shows that similar semiconductor devices has similar radiation susceptibility, so a method to assess the radiation effects on semiconductor devices base on similarity theory is proposed at first time in this paper. This assessing method does not require irradiation testing and does not require separate sampling. It has the virtues of easy implementation, quick response and low cost, providing an efficient method of assessing radiation effects on semiconductor devices.

**Keywords**—*semiconductor devices; semiconductor and devices physics ; physical mechanisms; radiation effects; radiation susceptibility;similarity principle*

## I. INTRODUCTION

Electronic parts in space applications inevitably subject to radiation effects leading to the degradation of electronic performance or even failure, especially for semiconductor device[1]. Space radiation effects include cumulative effects such as total ion dose(TID) and displacement damage dose (DDD), and transient effects such as single event latchup(SEL), single event upset(SEU), single event transient(SET), single event burnout(SEB), single event gate rupture(SEGR) and *etc*, which can reduce the performance of semiconductor devices or directly lead to failure, Therefore, it is necessary to know the radiation susceptibility of the semiconductor devices in order to ensure their reliability in aerospace applications[2].

At present, the acquisition of radiation susceptibility of semiconductor devices is completed through irradiation tests on the ground, irradiating  $\gamma$ -rays, protons, neutrons, and high-energy charged particles directly to semiconductor devices. Due to cyclotron is rare and it runs only a few months a year, so the test time is difficult to appoint and the cost is huge,

which cannot conduct irradiation testing on all semiconductor devices in space missions and meet the mission development progress. This has caused difficulties in evaluating the radiation susceptibility of semiconductor devices applied in aerospace, especially in commercial aerospace missions.

The single event effect(SEE) simulation experiment using laser pulse is another fast and economical method to obtain the radiation susceptibility of semiconductor devices. However, due to the limitation of the range of light pulses within the semiconductor devices, the equivalence of their results with cyclotron heavy ion tests has not been fully recognized [3]. In practical, laser pulse simulation experiments are a good method to verify the effectiveness of radiation hardening.

The irradiation test data shows that semiconductor devices with the similar function have similar radiation susceptibility. The TID and SEL performance of Xilinx Virtex-4 FPGA, the SEL and DDD performance of four COMS image sensors from COMSIS, the DDD susceptibility of 5 semiconductor laser Diodes from five manufacturers and the SEL susceptibility of 3 ADCs from ADI are shown in table 1, table 2, table 3 and table 4, respectively. These irradiation test data are partly from [2] [4] [5] [6], and partly from the irradiation tests of Chinese space missions. Table 1, table 2, table 3 and table 4 provide a suggestion that semiconductor devices with the same or similar function may have the same or similar radiation susceptibility. Therefore, the similarity in design topology and manufacturing technology of semiconductor devices can be used to assess their radiation susceptibility. This assessment technique based on the similarity theory does not require cyclotron testing, nor does it require separate sampling. It has the virtues of easy implementation, quick response and low cost, providing an efficient method of assessing radiation effects on semiconductor devices.

Table 1. Radiation performance of Xilinx V4 FPGA

Device		TID (krad Si)	SEL LET <sub>TH</sub> (MeV-cm <sup>2</sup> /mg)
XC4VFX60	90nm, bulk process	>300	>75
XC4VLX60	90nm, bulk process	>300	>75
XC4VSX35	90nm, bulk process	>300	>75
XC4VSX55	90nm, bulk process	>300	>75
XOR4V55	90nm, EPI process	>300	>109
XOR5V55	65nm, EPI process	>1M	>125

Table 2. Radiation performance of COMSimage sensors from COMSIS

Device		SEL LET <sub>TH</sub> (MeV·cm <sup>2</sup> /mg)	DDD (p/cm <sup>2</sup> )
CMV2000	5.5 μm/pixle	<14	10 <sup>11</sup>
CMV4000	5.5 μm/pixle	9.3-13.2	10 <sup>11</sup>
CMV12000	5.5 μm/pixle	<14	10 <sup>11</sup>
CMV20000	6.4 μm/pixle	<15	>4.1*10 <sup>10</sup>

Table 3. Radiation performance of Laser Diodes

Device	Manuf.	Technology	λc (nm)	DDD (p/cm <sup>2</sup> )
BMUT5-915-02-R	Oclaro	GaAs	915	10 <sup>11</sup>
JDSU-30-7602-660	JDSU	GaAs	976	10 <sup>11</sup>
K808D06FA-4.00W	BWT Beijing	GaAs	808	10 <sup>11</sup>
CP-405-PLR-40-2	OndaxInc	GaAs	405	10 <sup>11</sup>
QLD-808-150S	Qphotonics	GaAs	808	10 <sup>11</sup>

Table 4. Radiation performance of 12-bit ADC from ADC

Device	topology	Technology	SEL LET <sub>TH</sub> (MeV·cm <sup>2</sup> /mg)
AD7854	SAR	CMOS	6.7<<11.4
AD7858	SAR	CMOS	11.4<<22.8
AD7888	SAR	CMOS	16.7<<22.8

The similarity theory has been extensively studied and applied [7] [8] [9] [10]. For example, in the field of fluid mechanics, an aircraft is too large to directly study the flight problems in wind tunnel, and insects is too small to conduct wind blowing experiments directly in wind tunnels. So the most concerning question is whether the physical phenomena described from the experimental results of the model can truly reproduce the original physical phenomena? If the accurate quantitative data obtained from model experiments can accurately represent the flow phenomenon of the corresponding prototype, the following similarities must be met between the model and the prototype. These lead to the similarity theory, including the first and second theorems of similarity.

Similar physical phenomena must follow the same objective laws. If these laws can be expressed by equations, the physical equations must be exactly the same, and the corresponding similarity criteria must have equal numerical values. This is the first theorem of similarity. It is worth noting that a physical phenomenon has different values for similarity criteria at different times and spatial positions, while similar physical phenomena have equal values for similarity criteria at corresponding times and points. Therefore, similarity criteria are not constants. If two physical phenomena are similar, they must be of the same type. Therefore, the system of differential equations describing physical phenomena must be the same, which is the first necessary condition for phenomenon similarity. Single valued condition similarity is the second necessary condition for physical phenomenon similarity. Because there are many phenomena of the same kind that follow the same system of differential equations, the single value condition can distinguish the research object from countless phenomena, and mathematically it is a definite solution condition that makes the system of differential equations have a unique solution. The similarity criterion consisting of physical quantities in a single value condition is equal, which is the third necessary condition for phenomenon similarity. On the other hand, when belonging to the same class of physical phenomena and having similar single value

conditions, two phenomena only have a corresponding relationship in time and space, as well as the same physical quantities related to time and space. If the corresponding similarity criteria are equal and the physical quantities at the corresponding time and space points are maintained at the same ratio, it ensures the similarity of the two physical phenomena. In summary, the similarity condition can be expressed as: for the same type of physical phenomenon, when the similarity criteria composed of physical quantities in the single valued condition are equal and the single valued conditions are similar, then these phenomena must be similar. This is the second theorem of similarity, which is a necessary and sufficient condition for determining whether two physical phenomena are similar.

In mathematics, the similarity between two similar systems can be expressed as the existence of feature or attribution with the same components or elements but different in values. Suppose two similar systems  $X$  and  $Y$ , where  $X$  has a total of  $a$  attributions  $x_1, x_2, \dots, x_a$ , and  $Y$  has a total of  $b$  attributions  $y_1, y_2, \dots, y_b$ . If the  $x_i$  in  $X$  and the  $y_j$  in  $Y$  have the same attributions, then  $x_i$  and  $y_j$  are similar to each other.

Assuming that the similarity attribution  $z$  constituting of  $x_i$  and  $y_j$  has  $n$  elements  $e_1, e_2, \dots, e_n$ , the classic similarity attribution calculation formula is:

$$S(z) = w_1 e_1 + w_2 e_2 + \dots + w_n e_n = \sum_{i=1}^n w_i e_i \quad (1)$$

In(1),  $e_i$  is a element of the similarity attribution  $z$ ,  $w_i$  is the weighting coefficient of  $e_i$ , which satisfies  $0 \leq e_i \leq 1$ ,  $0 \leq w_i \leq 1$ ,  $w_1 + w_2 + \dots + w_n = 1$ ,  $0 \leq S(z) \leq 1$ .

Suppose the attribution numbers of systems  $X$  and  $Y$  are  $a$  and  $b$  respectively, and the number of similar attributions is  $m$ ,  $z_1, z_2, \dots, z_m$ , then the overall similarity of the system  $X$  and  $Y$  is:

$$S(X, Y) = \frac{m}{a+b-m} \sum_{i=1}^m w_i S(z_i) \quad (2)$$

In(2),  $S(z_i)$  represents the similar value of the  $i$ -th similar attribution, and  $w_i$  is the weight coefficient of it, which satisfies:  $0 \leq w_i \leq 1$ ,  $w_1 + w_2 + \dots + w_m = 1$ ,  $S(X, Y) \leq 1$ .

For example, for bipolar transistors (BJTs), their similar attributions include current amplification function, power amplification function, and switching function. The current amplification attribution has two similar elements, the common base current amplification factor  $\alpha$  and the common emitter current amplification factor  $\beta$ . Generally, the weight coefficients are set by application requirements and the experience of engineers, such as the space radiation effect on the current amplification factor  $\beta$  is significant, therefore its corresponding weight coefficient will be higher.

The basic components of semiconductor device is the PN junction, BJTs, and MOS transistor. The basic component of logic devices is the logic NOT composed of NMOS and PMOS transistors. The differential equation of the relationship between Fermi level and electric field is describing the physical properties of these basic component [11] [12] [13]. The physical mechanism of radiation effect is that high-energy particles enter devices and change the Fermi level, leading to changes in the performance parameters of devices [1]. Regardless of the type of device, the physical mechanism of

its radiation susceptibility is the same, and the impact on parameters is also single valued, thus belonging to the same physical phenomenon.

The second section of the paper discusses in detail the physical mechanism for assessing the radiation susceptibility based on the principle of similarity, which includes semiconductor physics, semiconductor device physics, topology and technology, to ensure that the radiation susceptibility of semiconductor devices comply with the first and second theorems of similarity. The third section of the paper introduces a specific method for assessing the radiation susceptibility based on similarity. The fourth section of the paper presents an application cases, and finally concludes with conclusions and discussions.

## II. PHYSICAL MECHANISM OF RADIATION

### SUSCEPTIBILITY ASSESSMENT BASE ON SIMILARITY THEORY

#### A. The physical mechanism of semiconductor devices

The motion of charge carriers inside semiconductor device under the external electric field can be described by a set of basic equations, which are derived from Maxwell's equations combined with the solid-state physical, including Poisson's equation, current density equation, and continuity equation. The physical description of semiconductor device can be found in any textbook or lecture on semiconductor physics and semiconductor device physics. Here are some relevant conclusions [11] [12] [13].

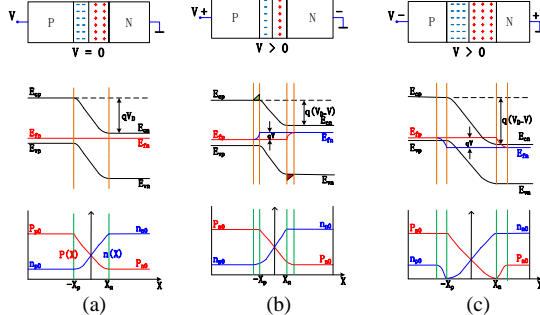


Fig.1 Energy band in silicon bandgap of a PN junction

The basic element of semiconductor devices is the PN junction, where the drift and diffusion of electrons and holes are related to the Fermi energy level and its position between the conduction band bottom and the valence band top. The Fermi energy levels of a PN junction in equilibrium are equal everywhere, and in order to achieve equal Fermi energy levels, the entire valence band in the P region needs to be shifted up  $E_{fn}-E_{fp}$  relative to the valence band in the N region. This energy difference is actually caused by the potential difference of the electric field in the charge region, as shown in Figure 1 (a). Note that the top of the valence band and the bottom of the conduction band in the charge region of the band diagram are curves rather than straight lines, which are for the convenience of drawing. When an electric field is applied to the PN junction, the energy band undergoes a change. The first scenario is to add a forward voltage - connect the P zone to a

high voltage and the N zone to a low voltage. The direction of the external electric field is opposite to the original direction of the internal electric field in the charge region, weakening the original electric field and causing a decrease in the height of the potential barrier. The diffusion flow is greater than the drift flow, so there will be non-equilibrium minority electrons diffusing from the N region to the P region, as well as non-equilibrium minority holes diffusing from the P region to the N region. They form a pile up on the outer side of the charge region, triggering diffusion currents inside the P and N regions. The second scenario is to add a reverse voltage - connect the P region to a low voltage and the N region to a high voltage. The external electric field enhances the internal electric field in the charge region and suppresses the diffusion of non-equilibrium minority carriers. The PN junction energy band diagrams with applied forward and reverse voltages are shown in Figure 1 (b) and Figure 1 (c).

In the differential equations of semiconductor devices introduced below, the focus is on the relationship between electrical performance, material parameters, geometric parameters, and process parameters, ignoring the specific meaning of the subscripts.

The carrier concentrations  $n_0$  and  $p_0$  in the equilibrium PN junction follow a Boltzmann distribution and are determined by the valence band  $E_V$ , conduction band  $E_C$ , Fermi energy level  $E_F$ , and doping concentration  $N_C$  and  $N_p$ :

$$n_0 = N_C \exp[-(E_C - E_F)/kT]$$

$$p_0 = N_V \exp[-(E_F - E_V)/kT]$$

Therefore, the current-voltage equation of an ideal PN junction derived from Poisson's equation, current density equation, and continuity equation is:

$$J = J_p + J_n = J_s \left( e^{qV/kT} - 1 \right)$$

Here  $J_n$ :

$$J_n = -q\mu_n N_C \exp\left(\frac{E_F - E_C + qV}{kT}\right) \frac{dV}{dx} + qD_n \frac{d}{dx} \left[ N_C \exp\left(\frac{E_F - E_C + qV}{kT}\right) \right] \quad (3)$$

It can be seen that  $J_n$  is related to external electric field  $V$ , and also related to material parameters such as  $E_F$ ,  $E_C$ ,  $u_n$  and  $D_n$ , geometric parameters such as  $x$ , and the process parameters such as  $N$ . So is  $J_p$ .

For BJTs, the key parameter is the common base current amplification factor  $\alpha$  and the common emitter current amplification factor  $\beta$ . It can be expressed as:

$$\alpha \approx \left[ 1 - \frac{W_b^2}{2L_{nb}^2} \right] / \left[ 1 + \frac{\rho_e W_b}{\rho_b L_{pe}} \right] \approx 1 - \frac{\rho_e W_b}{\rho_b L_{pe}} - \frac{W_b^2}{2L_{nb}^2} \approx 1 \quad (4)$$

$$\beta = \frac{\alpha}{1-\alpha} \approx \frac{1}{1-\alpha} = \left[ \frac{\rho_e W_b}{\rho_b L_{pe}} + \frac{W_b^2}{2L_{nb}^2} \right]^{-1} \gg 1 \quad (5)$$

For field-effect transistors, the key parameter threshold voltage  $V_T$  can be expressed as:

$$V_T = (q\phi_g - q\phi_t - \frac{Q_0}{C_{ox}}) \pm \left( \frac{qN_a x dT}{C_{ox}} + 2 \frac{kT}{q} \ln \frac{N_a}{n_i} \right) \quad (6)$$

In (6),  $Q_0$  is charge quantity, potential  $\Phi$  It is corresponding to the change in Fermi level,  $C_{ox} = \epsilon_r \epsilon_0 S / t_{ox}$  is the oxide layer capacitance related to the geometric parameters ( $S$ ,  $t_{ox}$ ) and material parameters ( $\epsilon$ ).

Ignoring the specific meaning of the subscripts in (3), (4), (5), and (6), it can be seen that the electrical performance of semiconductor devices are determined by the material parameters ( $D$ ,  $\epsilon$  and  $\rho$ ), and the geometric parameters ( $W$ ,  $L$ ,  $S$ , and  $t_{ox}$ ). and the process parameters ( $N$ ,  $n$ ). The material and geometric parameters are jointly determined by the design topology and the manufacturing technology. So, semiconductor devices with the same or similar topology and technology should have the same or similar electrical properties

### B. The physical mechanism of radiation effects

Radiation effect is a complex phenomenon that can be divided into ionizing radiation effect and non ionizing radiation effect. Ionizing radiation is mainly caused by the interaction between charged particles and atoms in the device, causing atoms to deviate from their original charged state and internal energy, resulting in atomic ionization. Ionization effect should include the main manifestations of total dose effect and single event effect (SEE). SEE includes SEL, SEU, SET, SEB and SEGR. The non ionizing radiation effect refers to the long-term effects of high-energy particles such as protons, neutrons, and nuclear fragments, which mainly cause the lattice atoms of the semiconductor device to deviate from their original positions and produce vacancies, substitutions, or more complex complexes, introducing defects and traps can have long-term effects on semiconductor devices.

A systematic study has been conducted on the physical mechanism of irradiation effects [1] [14] [15] [16] [17] [18] [19]. In [1] [14] [15], for bipolar transistors and field-effect transistors, charged particles alter their current voltage characteristics by affecting the Fermi level of surface states, as shown in Figure 2. Specifically, ionization in the intrinsic and extrinsic base regions of bipolar transistors, as well as the  $SiO_2-Si$  interface of field-effect transistors, introduces hole trapping and electron charging charges, which change the potential corresponding to the Fermi level. In other words, the potential term is added to the expressions for transistor current amplification and field-effect transistor threshold voltage, resulting in changes in electrical performance. If the charges generated by these irradiation persist for a long time, it leads to a degradation of electrical performance.

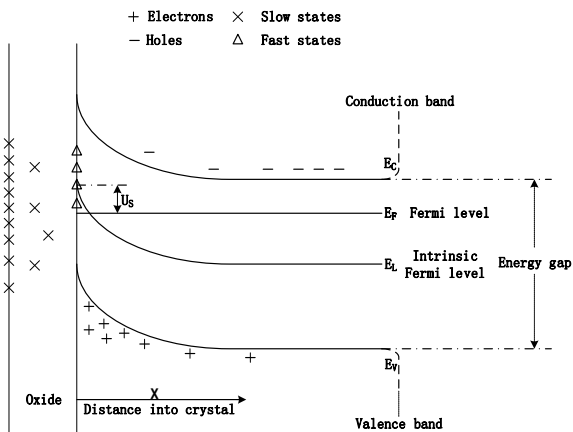


Fig.2 Band structure at the surface of a semiconductor.

In [1] [16] [18] [19], the mechanism of single event latchup is that parasitic PNP and NPN transistors form a thyristor circuit during the manufacturing process of CMOS devices, as shown in Figure 3. Under the condition that the product of the current amplification factor of the parasitic npn and pnp transistors is greater than 1, i.e.  $\beta_{npn} \beta_{pnp} > 1$ , when the thyristor circuit is triggered and the current latch-up occurs, which disrupts the normal operation of the CMOS circuit.  $\beta_{npn}$  and  $\beta_{pnp}$  is described using differential equation (5), and the substrate resistance  $R_s$  and well resistance  $R_w$  is also determined by geometric parameters and process parameters.

When charged particles in space generate a voltage drop on the substrate resistance  $R_s$  or well resistance  $R_w$ , or inject current into the base of the parasitic transistor, it triggers the parasitic thyristor to the latchup state.

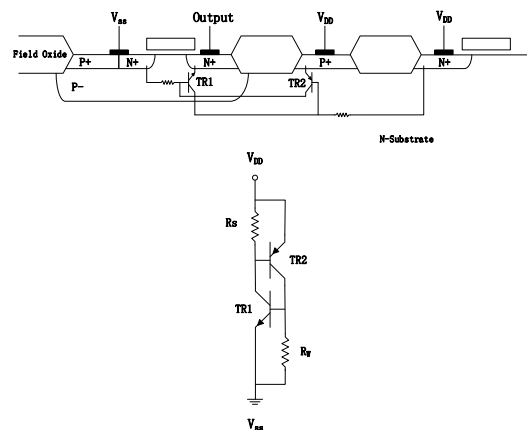


Fig.3 The npn electrical latchup structure in CMOS

### C. Applicability of similarity theory

From the semiconductor device physics and the physical mechanisms of the radiation effects discussed above, it can be seen that the current and voltage characteristics of different diodes, bipolar transistors, and field-effect transistors follow the same semiconductor physical laws and are described using the same physical equations. Also, the radiation effect on the semiconductor devices still follows these physical laws, and the electrical performance parameters and radiation susceptibility are the same under the same topology and technology, thus meeting the requirements of the first theorem of similarity. At the same time, the physical quantities in the physical equations are defined the same, and the solution to the equation under given topology and technology is unique, thus meeting the requirements of the second theorem of similarity. So that is, the principle of similarity is applicable to the assessment of radiation susceptibility of semiconductor devices.

## III. METHODS OF RADIATION SUSCEPTIBILITY ASSESSMENT BASE ON SIMILARITY THEORY

Although the physical mechanism of the radiation effects on semiconductor devices is the same, different topology and technology determine different radiation susceptibility. For example, the SEL  $LET_{th}$  of Samsung's 0.35um process C-

version 4M SDRAM (K6R4008C1C) is great than 37MeV-cm<sup>2</sup>/mg, while the SEL  $LET_{th}$  of 0.18um process D-version 4M SDRAM (K6R4008C1D) is less than 1 MeV-cm<sup>2</sup>/mg[20]. Due to the uncertainty and errors introduced in the manufacturing process, it is difficult to directly obtain the radiation susceptibility of a semiconductor device using physical models. At the same time, it is also difficult for end-users to obtain detailed topology and technology parameters. Therefore, in practical space applications, a combination of model analysis and experimentation is used. So the topology and technology of a semiconductor device, and the accumulated irradiation test data are the basis for achieving the assessment of radiation susceptibility.

The method for assessing the radiation susceptibility based on similarity principle is to obtain the topology and technology information of the semiconductor device to be assessed as much as possible, and compare it with the topology and technology information of the semiconductor device with known radiation susceptibility. When the similarity between the two is greater than the criteria of the requirements, it can be considered that the radiation susceptibility of the one to be assessed is similar to the known one.

The methods for assessing the radiation susceptibility based on similarity introduced here is to integrate technical means such as topology and technology information analysis, big data, and similarity analysis. This mainly includes the following steps:

- 1) Retrieve the topology and technology information of the semiconductor device to be assessed that have the same or similar functions as the known one through database, including but not limited to the functions, performance, topology, quality level, manufacturing technology information (technology note, substrate material, CMOS/bipolar, layout, epitaxial layer thickness, isolation well, isolation ring, transverse/longitudinal junction, homogeneous/heterojunction, well source structure, diffusion resistance, etc.) as much as possible.
- 2) Obtain the technology information of the semiconductor device to be assessed and the known one by construction analysis. That is, to use focused ion beam (FIB), scanning electron microscope (SEM) and other instruments to obtain the manufacturing technology information which not available in step 1.
- 3) Similarity analysis, that is, to calculate the similarity value of the one to be assessed and the known one using (1) and (2), and the similarity analysis table is shown in the table 5.

Table 5. Analysis table of similarity value S

Attributes/ elements	topology				technology			
	Manuf.	function	building blocks	...	foundry	note	process	...
known								
to be assessed								
weight								
elements S								
total S								

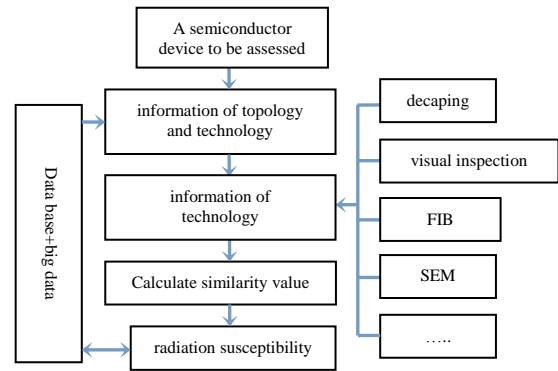


Fig.4 Flow chart of assessing radiation susceptibility of a semiconductor device based on similarity theory

If the similarity value calculated by analyzing Table 4 is  $s$ , then one can say that the radiation susceptibility of a semiconductor device to be assessed is similar to the known one with the confidence levels.

4) Summarize the assessed results and input them into the database for updating, providing data support for subsequent radiation susceptibility assessment.

The flowchart of assessing radiation susceptibility based on similarity theory is shown in figure 4.

#### IV. A CASE OF RADIATION SUSCEPTIBILITY ASSESSMENT

A DAC converter TLV5638 from TI was selected to be used in a Chinese space science mission, ShiJian 10, conducted by CAS, and at that time, only the irradiation test data of DAC converters TLV5618, TLV5636, and TLV5616 were available. The  $LET_{th}$  of SEL of TLV5618 was about 5 MeV cm<sup>2</sup>/mg [21], and the  $LET_{th}$  of SEL of TLV5636 and TLV5616 was both greater than 200 MeV cm<sup>2</sup>/mg (last test) [2]. TLV5636 and TLV5616 both is a single 12-bit voltage output DAC implemented with a CMOS process. TLV5636 is almost assume as TLV5616 except for its shorter programmable settling time and a built-in reference source [22] [23]. TLV5638 and TLV5618 both is a dual 12-bit voltage output DAC implemented with a CMOS process. TLV5638 is almost as same as TLV5616 except for its shorter programmable settling time and a built-in reference source [24] [25]. The functions of TLV5636 and TLV5616 are the same, with the same electrical characteristics and SEL performance, indicating a high degree of similarity. So it is reasonable to speculate that TLV5638 and TLV5618 have similar radiation susceptibility, as their functions is the same and their electrical characteristics is almost the same.

The similarity analysis for TLV5638 and TLV5618 was conducted according to the similarity analysis methods as mentioned in Section III.

1) The functional attributes and their elements, circuit architecture attributes and their elements, and electrical performance attributes and their elements, obtained from the TLV5638 and TLV5618 data sheets, are shown in Tables 6, 7, and 8, respectively.

Table 6.Elements of function attribute

Attribute Elements	Function		Weight factor
	5638	5618	
e <sub>1</sub>	Dual 12-Bit Voltage Output DAC	Dual 12-Bit Voltage Output DAC	1/6
e <sub>2</sub>	Programmable Internal Reference	-	1/6
e <sub>3</sub>	Programmable Settling Time	Programmable Settling Time	1/6
e <sub>4</sub>	Compatible With TMS320 and SPI™ SerialPorts	Compatible With TMS320 and SPI SerialPorts	1/6
e <sub>5</sub>	Differential Nonlinearity <0.5 LSB Typ	Differential Nonlinearity <0.5 LSB Typ	1/6
e <sub>6</sub>	Monotonic Over Temperature	Monotonic Over Temperature	1/6

Table 7.Elements of topology block attribute

Attribute Elements	Topologyblock		Weight factor
	5638	5618	
e <sub>1</sub>	Power-On Reset	Power-On Reset	1/8
e <sub>2</sub>	Power and Speed Control	Power and Speed Control	1/8
e <sub>3</sub>	Programmable Internal Reference	-	1/8
e <sub>4</sub>	Serial Interface and Control	Serial Interface and Control	1/8
e <sub>5</sub>	Buffer	Buffer	1/8
e <sub>6</sub>	12-Bit DAC A and B Latch	12-Bit DAC A and B Latch	1/8
e <sub>7</sub>	resistor string	resistor string	1/8
e <sub>8</sub>	x2 output buffer	x2 output buffer	1/8

Table 8.Elements of Electrical Characteristics attribute

Attribute Elements	Electrical Characteristics	Electrical Characteristics		Weight factor
		5638	5618	
e <sub>1</sub>	I <sub>HH</sub>	Max 1	Max 1	1/22
e <sub>2</sub>	I <sub>HL</sub>	Min -1	Min -1	1/22
e <sub>3</sub>	C <sub>i</sub>	TYP 8	TYP 8	1/22
e <sub>4</sub>	t <sub>i</sub> (FS)	TYP 1	TYP 1	1/22
e <sub>5</sub>	t <sub>i</sub> (CC)	TYP 0.5	TYP 1	1/22
e <sub>6</sub>	SR	TYP 12	TYP 3	1/22
e <sub>7</sub>	.....	.....	.....	1/22
e <sub>21</sub>	t <sub>on</sub> (D)	Min 10	Min 5	1/22
e <sub>22</sub>	t <sub>o</sub> (D)	Min 5	Min 5	1/22

2) The interface, buffer, 12-Bit DAC latch and output amplification region in the die of TLV5638 and TLV5618 were analyzed using FIB and SEM, respectively. The elements of fabricate process attribute of different functional regions were obtained in Table 9. The cross-section SEM photography of the 12-Bit DAC latch region and gate region are shown in Figure 5.

Table 9.Elements of fabricate process attribute

Elements	Attribute	fabricate process		Weight factor
		5638	5618	
e <sub>1</sub>	technology	CMOS bulk	CMOS bulk	1/7
e <sub>2</sub>	node	0.8um	0.8um	1/7
e <sub>3</sub>	thickness of SiO <sub>2</sub> of gate	0.28um	0.28um	1/7
e <sub>4</sub>	Metal layers	2	2	1/7
e <sub>5</sub>	transverse/longitudinal junction	transverse	transverse	1/7
e <sub>6</sub>	homogeneous/heterojunction	homogeneous	homogeneous	1/7
e <sub>7</sub>	isolation ring	no	no	1/7

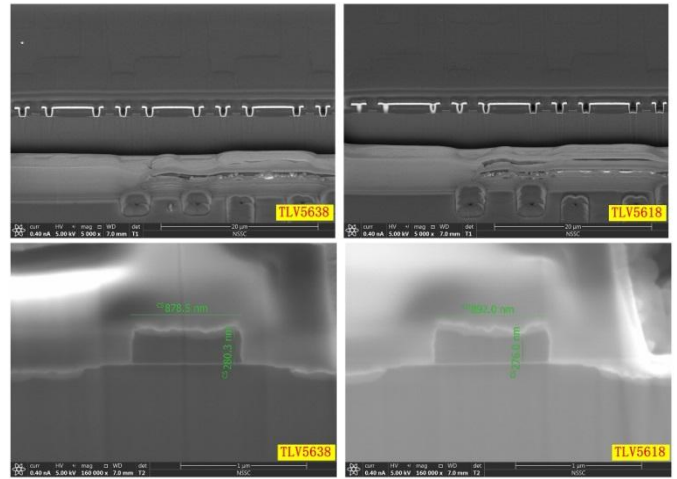


Fig.5 SEM photography of the cross section of 12-Bit DAC latch and gate region.(left)TLV5638,(right)TLV5618.

3) Tables 6, 7, 8, and 9 constitute the similarity analysis table shown in Table 5. According to the calculations in (1) and (2), the similarity between TLV5638 and TLV5618  $S(TLV5638, TLV5618) \approx 0.89$ . Therefore, it can be considered that the LET<sub>th</sub> of SEL of TLV5638 is as the same order as TLV5618, which is less than 10 MeV-cm<sup>2</sup>/mg. So TLV5638 is very susceptible to SEL and a mitigation method should be used to ensure its reliability in the space mission, for example, the method of serially connecting a current limiting resistor *r* between the power supply and V<sub>DD</sub> as shown in Figure 6

4) Import the data from steps 1, 2, and 3 into the database to provide data support for subsequent radiation susceptibility analysis.

A verification test of the mitigation method shown in figure 6, which a resistor *r* is connected in series between the power supply and the V<sub>DD</sub> pin, was conducted after TLV5638 worked normally in the space mission ShiJian 10. Under the irradiation of Ge ions (LET=37.3 MeV-cm<sup>2</sup>/mg), TLV5638 showed multiple occurrences of latchup[26], indicating that TLV5638 is very sensitive to SEL and directly verifying the assessment of SEL performance of TLV5638 based on similarity principle.

After the verification test of the mitigation method as shown in figure 6, TLV5638 was also used successfully in Chinese space science mission Advanced Space-based Solar Observatory (ASO-S) and Chinese Mars mission, further validated the effectiveness of applying similarity theory to evaluate irradiation susceptibility.

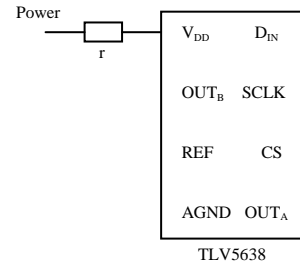


Fig.6 A mitigation method of current limitation

## V. CONCLUSION

In this paper, based on semiconductor physics, semiconductor device physics and the physical mechanism of radiation effect, the possibility of applying similarity theory to assess the radiation susceptibility of semiconductor devices is proven, and a specific evaluation method and application case is presented.

The effectiveness of assessing radiation susceptibility based on the similarity theory depends on the acquisition and determination of similarity attributes and elements, as well as the determination of similarity values. In practical applications, it is often difficult for end-users or quality assurance agencies to obtain all the required similar information, and also, the mathematical algorithms for calculating the similar values and the acceptance criteria also require engineers to determine based on experience and application requirements.

## REFERENCES

- [1] C. Claeys, and E. Simoen, *Radiation Effects in Advanced Semiconductor Material and Devices*, 2002 Springer, ISBN 978-7-118-05408-8.
- [2] *Guideline for the Selection of COTS Electronic Parts in Radiation Environments*, NASA, 2019.
- [3] V. Pouget, H. Lapuyade, *et al.*, "Theoretical Investigation of an Equivalent Laser LET," *Microelectronics Reliability* 41(2001) 1513-1518.
- [4] C. Poivey *et al.*, "Single Event Effects (SEE) response of embedded power PCs in a Xilinx Virtex-4 FPGA for a space application," *2007 9th European Conference on Radiation and Its Effects on Components and Systems*, Deauville, France, 2007, pp. 1-5, doi: 10.1109/RADECS.2007.5205563.
- [5] Adamice P, Barbero J, Moya A L, *et al.*, "Radiation tests on the COTS image sensor from CMOSIS," *International Conference on Space Optics-ICSO 2018*. SPIE 2019, 11180:2779-2786.
- [6] H. Liu *et al.*, "Displacement Damage Test on COST Laser Diodes Embedded in Satellite," *RADECS2015, Radiation Effects Data Workshop*.
- [7] Sandro G. Longo, *Principle and Applications of Dimensional Analysis and Similarity*, Springer, ISBN 978-3-030-79216-9
- [8] W. Chuanyuan, "Exploration and study on similarity theory," in *Journal of Systems Engineering and Electronics*, vol. 3, no. 1, pp. 9-20, March 1992.
- [9] L. B. Liu, R. Y. Qian, J. Li, M. G. Sun and S. C. Ge, "GPR detection of subsurface voids and its validation based on similarity principle," *2016 16th International Conference on Ground Penetrating Radar (GPR)*, Hong Kong, China, 2016, pp. 1-4, doi: 10.1109/ICGPR.2016.7572662.
- [10] T. Liang, X. Li, N. Wei, P. Xu and J. Wang, "Research on Similarity Evaluation Method of Complex Electromagnetic Environment Based on Similarity Theory," *2021 13th International Symposium on Antennas, Propagation and EM Theory (ISAPE)*, Zhuhai, China, 2021, pp. 1-4, doi: 10.1109/ISAPE54070.2021.9753462.
- [11] A. S. Grove, *Physics and Technology of Semiconductor Devices*. New York, NY: Wiley, 1967.
- [12] S. M. Sze, *Physics of Semiconductor Devices*, Second Edition. New York, NY: Wiley, 1981.
- [13] E. H. Nicollian and J. R. Brews, *MOS Physics and Technology*. New York, NY: Wiley, 1982.
- [14] J. R. Srouf and J. M. McGarrity, "Radiation effects on microelectronics in space," in *Proceedings of the IEEE*, vol. 76, no. 11, pp. 1443-1469, Nov. 1988, doi: 10.1109/5.90114.
- [15] J. P. Mitchell and D. K. Wilson, "Surface effects of radiation on semiconductor devices," in *The Bell System Technical Journal*, vol. 46, no. 1, pp. 1-80, Jan. 1967, doi: 10.1002/j.1538-7305.1967.tb02443.x.
- [16] F. W. Sexton, "Destructive single-event effects in semiconductor devices and ICs," in *IEEE Transactions on Nuclear Science*, vol. 50, no. 3, pp. 603-621, June 2003, doi: 10.1109/TNS.2003.813137.
- [17] P. E. Dodd and L. W. Massengill, "Basic mechanisms and modeling of single-event upset in digital microelectronics," in *IEEE Transactions on Nuclear Science*, vol. 50, no. 3, pp. 583-602, June 2003, doi: 10.1109/TNS.2003.813129.
- [18] J. C. Pickel, "Single-event effects rate prediction," in *IEEE Transactions on Nuclear Science*, vol. 43, no. 2, pp. 483-495, April 1996, doi: 10.1109/23.490895.
- [19] A. Al Youssef, L. Artola, S. Ducret, G. Hubert and F. Perrier, "Investigation of Electrical Latchup and SEL Mechanisms at Low Temperature for Applications Down to 50 K," in *IEEE Transactions on Nuclear Science*, vol. 64, no. 8, pp. 2089-2097, Aug. 2017, doi: 10.1109/TNS.2017.2726684.
- [20] T. E. Page and J. M. Benedetto, "Extreme latchup susceptibility in modern commercial-off-the-shelf (COTS) monolithic 1M and 4M CMOS static random-access memory (SRAM) devices," *IEEE Radiation Effects Data Workshop, 2005.*, Seattle, WA, USA, 2005, pp. 1-7, doi: 10.1109/REDW.2005.1532657.
- [21] F. Malou *et al.*, "Compendium of TID and SEL test results for various candidate spacecraft electronics," *2007 9th European Conference on Radiation and Its Effects on Components and Systems*, Deauville, France, 2007, pp. 1-8, doi: 10.1109/RADECS.2007.5205560.
- [22] www.ti.com, TLV5636, SLAS223C – JUNE 1999 – REVISED APRIL 2004.
- [23] www.ti.com, TLV5616C, TLV5616I SLAS152D – DECEMBER 1997 – REVISED APRIL 2004.
- [24] www.ti.com, TLV5638, SLAS225C – JUNE 1999 – REVISED JANUARY 2004.
- [25] www.ti.com, TLV5618A, SLAS230H – JULY 1999 – REVISED JULY 2002.
- [26] H. Lv *et al.*, "Experimental Study on Single Event Latch-up of a D/A Converter," *2019 3rd International Conference on Radiation Effects of Electronic Devices (ICREED)*, Chongqing, China, 2019, pp. 1-4, doi: 10.1109/ICREED49760.2019.9205160.